LETTER

doi:10.1038/nature10712

Ars2 maintains neural stem-cell identity through direct transcriptional activation of *Sox2*

Celia Andreu-Agullo[1], Thomas Maurin[1], Craig B. Thompson[2] & Eric C. Lai[1]

Fundamental questions remain unanswered about the transcriptional networks that control the identity and self-renewal of neural stem cells (NSCs), a specialized subset of astroglial cells that are endowed with stem properties and neurogenic capacity. Here we report that the zinc finger protein Ars2 (arsenite-resistance protein 2; also known as Srrt) is expressed by adult NSCs from the subventricular zone (SVZ) of mice, and that selective knockdown of *Ars2* in cells expressing glial fibrillary acidic protein within the adult SVZ depletes the number of NSCs and their neurogenic capacity. These phenotypes are recapitulated in the postnatal SVZ of *hGFAP-cre*::*Ars2*$^{fl/fl}$ conditional knockout mice, but are more severe. *Ex vivo* assays show that Ars2 is necessary and sufficient to promote NSC self-renewal, and that it does so by positively regulating the expression of *Sox2*. Although plant[1–3] and animal[4,5] orthologues of Ars2 are known for their conserved roles in microRNA biogenesis, we unexpectedly observed that Ars2 retains its capacity to promote self-renewal in *Drosha* and *Dicer1* knockout NSCs. Instead, chromatin immunoprecipitation revealed that Ars2 binds a specific region within the 6-kilobase NSC enhancer of *Sox2*. This association is RNA-independent, and the region that is bound is required for Ars2-mediated activation of *Sox2*. We used gel-shift analysis to refine the Sox2 region bound by Ars2 to a specific conserved DNA sequence. The importance of *Sox2* as a critical downstream effector is shown by its ability to restore the self-renewal and multipotency defects of *Ars2* knockout NSCs. Our findings reveal Ars2 as a new transcription factor that controls the multipotent progenitor state of NSCs through direct activation of the pluripotency factor *Sox2*.

Stem cells reside in most mammalian tissues throughout adult life, and contribute to normal homeostasis and repair after injury[6]. They are defined by their capacity to both self-renew and differentiate, thus perpetuating themselves while generating more committed daughter cells. Two major stem-cell niches exist in the adult brain, and these are found within the hippocampus and within the SVZ. Relatively quiescent NSCs give rise to actively proliferating transit-amplifying progenitors, which generate oligodendrocytes that are destined for the corpus callosum[7] and neuroblasts that migrate rostrally and differentiate into local interneurons in the olfactory bulb[8,9]. Much remains to be understood about the mechanisms and factors that control NSC self-renewal and multipotency[10].

Mammalian Ars2 was reported to be essential for cell proliferation, to be downregulated in quiescent cells, and to be required for the accumulation of several microRNAs (miRNAs) that are implicated in cellular transformation[4]. Unexpectedly, we observed that Ars2 expression in the adult SVZ did not correlate with proliferation, as $95 \pm 2\%$ of Ars2$^+$-positive (Ars2$^+$) cells lacked the proliferative marker Ki67. Moreover, Ars2 was present in only $7 \pm 2\%$ of Mash1$^+$ transit-amplifying progenitors (Supplementary Fig. 1b) and was absent from doublecortin (DCX)-positive (DCX$^+$) neuroblasts (Fig. 1a); these comprise the most highly proliferative cells in the SVZ. Ars2 was also absent from GFAP$^+$Nestin$^-$Sox2$^-$ astroglial cells and S100β$^+$ mature astrocytes (Supplementary Fig. 1). Instead, Ars2 was

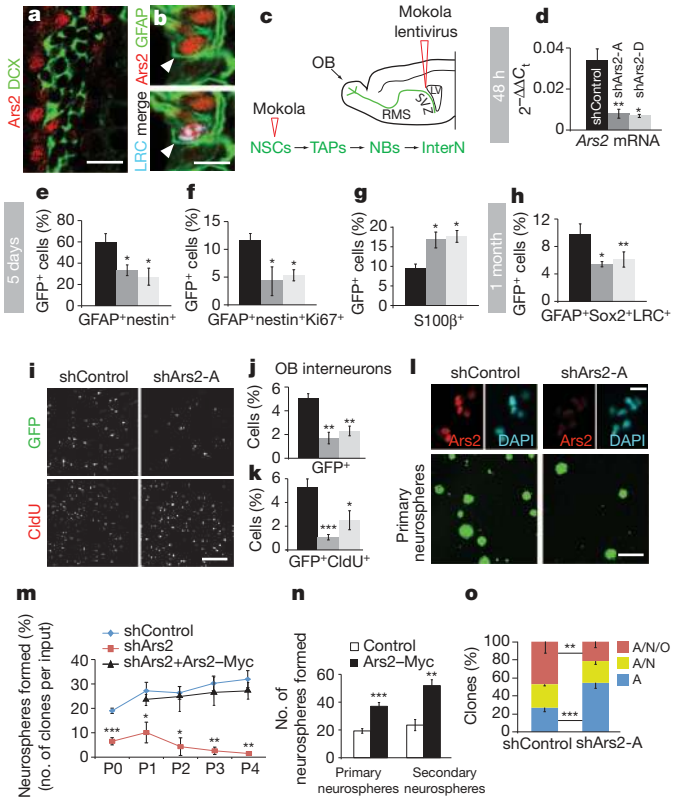

Figure 1 | Ars2 maintains neural stem cells in the adult SVZ. **a**, **b**, In the adult SVZ, Ars2 (red) is not expressed by DCX$^+$ (green) neuroblasts (**a**) but co-localizes with GFAP$^+$ (green), CldU-retaining (blue) NSCs (**b**). **c**, **d**, Experimental protocol (**c**) and validation of *Ars2* knockdown ($n = 3$ animals per condition) (**d**). **e**–**g**, *Ars2* knockdown in the SVZ exhibited reduced GFAP$^+$Nestin$^+$NSCs (**e**), reduced NSC proliferation (**f**) and increased S100β$^+$ mature astrocytes (**g**); $n = 3$ animals per condition. **h**, *Ars2* knockdown reduced LRCs ($n = 3$–7 animals per condition). **i**, Olfactory bulb sections double-stained for green fluorescent protein (GFP) and CldU. **j**, Percentage of GFP$^+$ cells per olfactory bulb slice ($n = 7$–11 animals per condition). **k**, Reduced newly generated neurons after *Ars2* knockdown ($n = 7$–11 animals per condition). **l**, Immunocytochemistry for Ars2 (red) and DAPI (4',6-diamidino-2-phenylindole; blue) (top) and GFP$^+$ transduced primary neurospheres (green; bottom). **m**, Long-term self-renewal assay ($n = 4$ cultures per condition). **n**, *In vivo* Ars2 overexpression increased neurosphere formation ($n = 4$ cultures per condition). **o**, Ars2 deficiency reduced NSC multipotency ($n = 4$ cultures per condition). A, astrocytes; InterN, interneuron; LV, lateral ventricle; N, neurons; NBs, neuroblasts; O, oligodendrocytes; OB, olfactory bulb; RMS, rostral migratory stream; TAPs, transit-amplifying progenitors. $^*P < 0.05$; $^{**}P < 0.01$; $^{***}P < 0.005$. Scale bars: **a**, **b**, 10 μm; **i**, 100 μm; **l**, 200 μm. Errors bars represent s.e.m. Supplementary Table 2 provides details of numbers of scored cells.

[1]Department of Developmental Biology, Sloan-Kettering Institute, 1275 York Avenue, Box 252, New York, New York 10065, USA. [2]Department of Cancer Biology and Genetics, Sloan-Kettering Institute, 1275 York Avenue, Box 252, New York, New York 10065, USA.

expressed by niche astrocytes, ependymal cells and GFAP$^+$CD133$^+$ stem cells[11] (Supplementary Fig. 1). A hallmark of NSCs is their quiescence, which is reflected in their ability to retain S-phase labels such as 5-chlorodeoxyuridine (CldU) for extended periods (that is, label-retaining cells (LRCs))[12,13]. We observed expression of Ars2 in 87 ± 3% of LRCs that were marked 1 month earlier (Fig. 1b), demonstrating the presence of Ars2 in this slow dividing population *in vivo*.

To assay the roles of Ars2 in NSCs *in vivo*, we used short hairpin RNAs (shRNAs) that suppressed endogenous Ars2 (Supplementary Fig. 2c). We packaged these into GFP-expressing Mokola lentivirus, which specifically transduces astroglial cells[14] (Supplementary Fig. 3). We used a defective lentivirus which is pseudotyped with a lyssavirus envelope of the Mokola virus. We injected these viruses into the adult SVZ and killed the mice 48 h, 5 days or 1 month later (Fig. 1c). At 48 h after infection, shArs2-GFP$^+$ cells exhibited an 80% reduction in *Ars2* messenger RNA relative to control shRNA cells (Fig. 1d). Apoptosis was unaffected by shArs2, and the number of GFP$^+$ Ki67$^+$ cells and the levels of cyclin D1 or cyclin E transcripts were also unchanged (Supplementary Figs 3, 4b and 5b). However, 5 days after infection, shArs2 SVZs exhibited a 50% reduction in the number and the proliferation rate of the GFAP$^+$Nestin$^+$NSCs (Fig. 1e, f), but apoptosis was unaffected (Supplementary Fig. 5b). Loss of NSC potential has been linked to an increase in mature astrocytes[15–17]. Consistent with this, we observed a 50% increase in the number of GFP$^+$S100b$^+$ cells (Fig. 1g).

To assess the number of LRCs, shRNA-infected mice were injected with CldU and killed 1 month later. Notably, we observed a decrease of ~50% in transduced LRCs in shArs2 SVZs (Fig. 1h), suggesting that Ars2 maintains the NSC pool. If this is true, we would expect it to have downstream effects on neurogenesis. Indeed, 5 days after infection, we observed a decrease in DCX$^+$ neuroblasts (Supplementary Fig. 6). LRCs also label post-mitotic cells that incorporate CldU just before cell cycle exit (such as differentiated cells and newly generated olfactory bulb interneurons). One month after infection, the population of shArs2-GFP$^+$, newly formed CldU$^+$ olfactory bulb interneurons was strongly reduced (Fig. 1i–k).

We performed additional analysis using neurospheres derived from shRNA-infected SVZ. Long-term self-renewal assays revealed that depletion of Ars2 rapidly extinguished neurosphere cultures, indicating a defect in self-renewing divisions (Fig. 1l, m). This defect was fully restored by an shRNA-resistant form of Ars2 (Fig. 1m and Supplementary Fig. 2d). Reciprocally, *in vivo* overexpression of Ars2 in wild-type mice increased neurosphere formation (Fig. 1n). Multipotency of Ars2-deficient neurospheres was also affected, as the frequency of clones that generated ßIII-tubulin$^+$ neurons and O4$^+$ oligodendrocytes was decreased in favour of unipotent GFAP$^+$ clones (Fig. 1o). We conclude that Ars2 is required to maintain NSCs in a self-renewing and multipotent state.

We sought to confirm these shRNA results by breeding the conditional knockout allele of *Ars2* (*Ars2$^{fl/fl}$*) with *hGFAP-cre* (ref.[18]). *hGFAP-cre::Ars2$^{fl/fl}$* mice (*Ars2$^{\Delta/\Delta}$* mice) (Supplementary Fig. 7d) were born at the expected Mendelian ratios relative to wild-type and *hGFAP-cre::Ars2$^{fl/+}$* littermates (used as controls). However, by postnatal day 15 (P15), *Ars2$^{\Delta/\Delta}$* mice showed progressive growth retardation, hydrocephalus and ataxia, resulting in death between P20 and P25. Further analysis of P15 *Ars2$^{\Delta/\Delta}$* mice revealed enlarged ventricles and smaller olfactory bulbs (Fig. 2a, b), suggestive of a requirement of Ars2 during postnatal neurogenesis. The expression pattern of Ars2 in P15 wild-type SVZ was analogous to the adult SVZ (Supplementary Fig. 7a,b), and analysis of the conditional knockout confirmed essentially complete absence of Ars2 in the SVZ (Supplementary Fig. 7c). Notably, the number of NSCs (marked by expression of nestin, Sox2, LeX (also known as Fut4) and GFAP) was reduced by 80% in *Ars2$^{\Delta/\Delta}$* SVZ, and their proliferation rate decreased twofold (Fig. 2c, d, f). Caspase 3 staining showed that this was not due to cell death (Supplementary Fig. 8a, b). Conversely, assessment by GFAP and S100β staining showed that there was marked astrogliosis in *Ars2$^{\Delta/\Delta}$* mice (Fig. 2e, f).

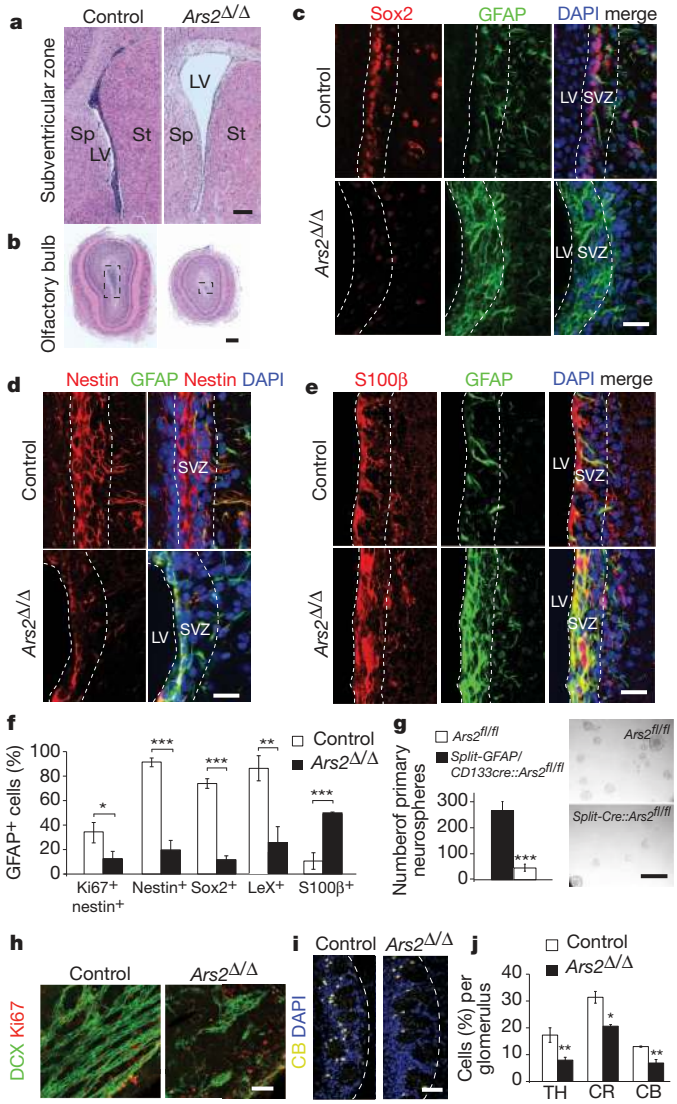

Figure 2 | Ars2 regulates postnatal neurogenesis. **a**, **b**, Coronal sections from P15 SVZ and olfactory bulb of control and *Ars2$^{\Delta/\Delta}$* mice, stained with haematoxylin and eosin. **c**–**e**, SVZ deletion of *Ars2* depleted NSCs and induced astrogliosis, as shown by loss of Sox2$^+$ (red) and accumulation of GFAP$^+$ (green) cells (**c**), loss of nestin$^+$ (red) cells (**d**), and increased S100β$^+$ (red) cells (**e**); DAPI is in blue. **f**, **g**, Reduced number and proliferation of NSCs and elevation of mature astrocytes in *Ars2$^{\Delta/\Delta}$* mice (**f**), and strong reduction of primary neurospheres from *GFAP/CD133-cre::Ars2$^{fl/fl}$* electroporated pups (**g**). **h**, Whole-mount immunostaining for DCX (green) and Ki67 (red). **i**, Olfactory bulb coronal sections immunostained for calbindin (CB; yellow) and DAPI (blue). **j**, Quantification of interneuron reduction in control and *Ars2$^{\Delta/\Delta}$* mice. CB, calbindin; CR, calretinin; TH, tyrosine hydroxylase. $*P < 0.05$; $**P < 0.01$; $***P < 0.005$. Scale bars: **a**, **b**, 100 µm; **c**–**e**, 30 µm; **g**–**i**, 50 µm. Error bars represent s.e.m from six animals per genotype or condition.

As Ars2 is expressed in niche astrocytes and ependymal cells, in addition to NSCs, we wished to demonstrate an autonomous function of Ars2 in NSCs. We co-injected GFP$^+$ and Split-Cre plasmids that specifically drive excision in GFAP$^+$CD133$^+$ NSCs[11] into the SVZ of P0–1 *Ars2$^{fl/fl}$* pups, and introduced these plasmids using electroporation. Five days later, we isolated GFP$^+$ cells and plated for self-renewal assay. GFAP$^+$CD133$^+$ NSCs deleted for *Ars2* were strongly compromised for neurosphere generation, demonstrating a cell-autonomous requirement of Ars2 in this population (Fig. 2g and Supplementary Fig. 9). Consistent with a decrease in the number of NSCs, *Ars2$^{\Delta/\Delta}$* mice had approximately 2.5-fold fewer DCX$^+$ neuroblasts (Fig. 2h) relative to control mice, although their proliferation rate was not affected (data not shown).

In the olfactory bulb, the frequency of tyrosine hydroxylase$^+$, calbindin$^+$ and calretinin$^+$ interneurons per glomerulus was also deeply reduced in *Ars2*$^{\Delta/\Delta}$ (Fig. 2i, j and Supplementary Fig. 10). In summary, the severe defects of the postnatal SVZ in which *Ars2* has been deleted solidified the requirement of Ars2 to maintain NSC identity.

As Ars2 functions in miRNA biogenesis[2–5], we tested whether the ability of Ars2 to promote NSC self-renewal was mediated by miRNAs. This was not the case, as overexpression of Ars2 in *Dicer1*$^{\Delta/\Delta}$ and *Drosha*$^{\Delta/\Delta}$ cells increased neurosphere yield (Fig. 3a,b). We sought to investigate this further by examining transcription factors that are known to have substantial roles in NSC self-renewal, including Hes1, Hes5 and Sox2 (refs 19–21). *Sox2* mRNA, but not *Hes1* mRNA, was significantly reduced 48 h after *Ars2* knockdown *in vivo* (Fig. 3c). One month after infection, *in vivo* knockdown of *Ars2* decreased *Hes1* and *Hes5* mRNA levels by ~30%, but resulted in a more substantial 70% reduction in *Sox2* (Fig. 3d). Reciprocally, *Sox2* levels increased by ~60% in neurospheres overexpressing Ars2 (Fig. 3e). These effects seemed to be transcriptional in nature, as Ars2 activated a 6-kilobase (kb) *Sox2-luc* reporter containing *cis*-regulatory sequences responsible for *Sox2* expression within adult neurogenic zones[22] (Fig. 3f). This was not simply due to the cancelling effects of overexpressing any self-renewal gene, because *in vitro* overexpression of Sox2 (Fig. 3g), but not Hes5 (Fig. 3h), rescued the Ars2-dependent loss in self-renewal capacity of shArs2 cells. Reciprocally, *in vitro* knockdown of *Sox2* (Supplementary Fig. 11a) caused rapid depletion of self-renewing neurospheres[23] (Fig. 3i) and compromised multipotency (Supplementary Fig. 11b), similar to the effects of *Ars2* knockdown (Fig. 1m, o). Together, these data indicated that Sox2 is a critical downstream effector of Ars2 in NSCs.

To evaluate whether the ability of Ars2 to activate *Sox2* expression might reflect a transcriptional role for this nuclear protein, we performed chromatin immunoprecipitation (ChIP) of Ars2 in NSCs, querying across the 6-kb *Sox2* promoter and the *Sox2* transcription unit. Interestingly, Ars2 associated not only with its 5′ untranslated region (UTR) and 3′ UTR but was highly enriched in region 8 (−2 to −2.5 kb) of the *Sox2* promoter (Fig. 4a); we validated this binding pattern using an independent antibody (Supplementary Fig. 12a). RNase treatment of chromatin samples eliminated UTR-associated Ars2 ChIP signals, and this is consistent with CBC-mediated association with capped transcripts[4]. However, binding of Ars2 to promoter region 8 was maintained, suggesting a more direct association of Ars2 with chromatin (Fig. 4b). No binding was found to the *Sox2* coding region (Fig. 4a) or to the promoters of *Hes1, Hes5* (ref. [24]), *K14* and *Myod1* (Supplementary Fig. 12b–e). Chromatin association of Ars2 was cell-type-dependent, as Ars2 did not bind the *Sox2* enhancer in NIH3T3 cells (Fig. 4a), which express high levels of Ars2 (Supplementary Fig. 2a).

Simple binding of Ars2 to the *Sox2* enhancer might not necessarily be of functional consequence. We prepared two deletions of the 6-kb *Sox2-luc* reporter, removing region 8 that was bound by Ars2 or region 5 as a

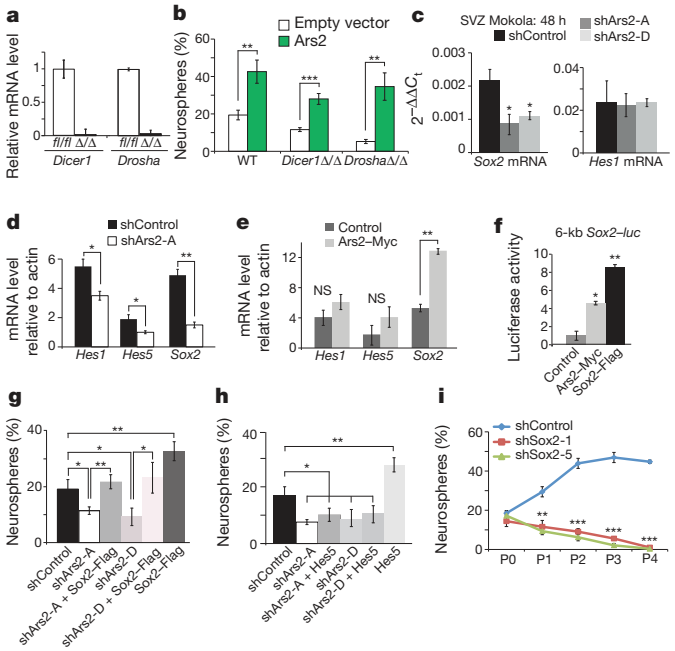

Figure 3 | Ars2 acts independently of the miRNA pathway to promote NSC self-renewal through *Sox2*. **a**, Absence of *Dicer1* and *Drosha* in floxed NSC cultures after Cre treatment ($n = 2$ experiments per condition). **b**, Ectopic Ars2 promoted NSC self-renewal in *Dicer1*- and *Drosha*-deleted NSCs ($n = 3$ experiments per condition). **c**, qPCR measurements from purified GFP$^+$ cells 48 h after infection ($n = 3$). **d**, qPCR measurements of self-renewal genes from primary infected GFP$^+$ NSCs ($n = 3$). **e**, Overexpression of Ars2 increased *Sox2* mRNA ($n = 3$). **f**, Both Ars2 and Sox2 activate a *Sox2* transcriptional reporter ($n = 3$). **g**, **h**, Percentage of neurospheres formed from NSCs infected with the indicated constructs ($n = 3$). **i**, Long-term self-renewal assay shows that Sox2 is required for NSC self-renewing divisions ($n = 4$). $^*P < 0.05$; $^{**}P < 0.01$; $^{***}P < 0.005$. Error bars represent s.e.m; NS, not significant; WT, wildtype.

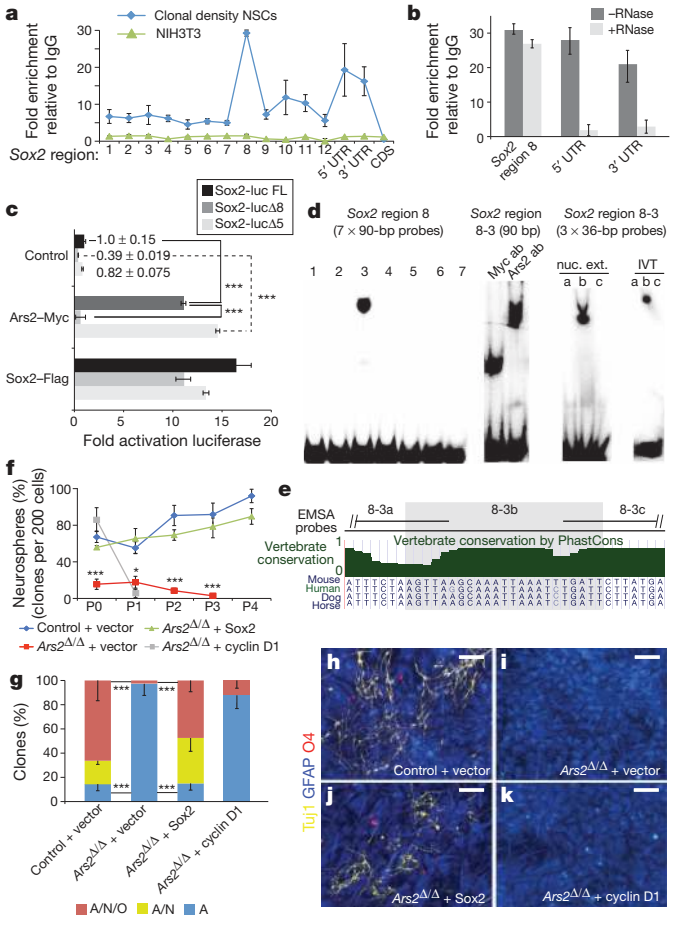

Figure 4 | Ars2 directly activates transcription of *Sox2* to mediate NSC self-renewal and multipotency. **a**, ChIP of Ars2 to the *Sox2* locus ($n = 4$ independent experiments). **b**, Ars2 binding to *Sox2* promoter region 8 is RNA independent ($n = 2$). **c**, Ars2 requires region 8 to activate *Sox2-luc* ($n = 4$). **d**, Gel shifts of the Ars2 binding site in the *Sox2* promoter using nuclear extract or *in vitro*-translated Ars2. **e**, Conservation of the Ars2-binding site in *Sox2*. **f**, Long-term self-renewal assay from NSCs isolated from control and *Ars2*$^{\Delta/\Delta}$ mice electroporated *in vivo* with the indicated constructs ($n = 6$ animals per condition). **g**, *Ars2*$^{\Delta/\Delta}$ defect in multipotency can be rescued by *in vivo* expression of Sox2 ($n = 6$ animals per condition). **h**–**k**, Differentiated NSC colonies stained for GFAP (blue), mouse anti-β-tubulin (Tuj1, yellow) and O4 (pink). Ab, antibody; bp, base pairs; CDS, coding sequence; EMSA, electrophoretic mobility shift assay; FL, full length; IVT, *in vitro*-translated; Luc, luciferase; Nuc. ext, nuclear extract; UTR, untranslated region;. $^*P < 0.05$; $^{***}P < 0.005$. Error bars represent s.e.m. Scale bars: **h**–**k**, 50 μm.

control deletion. Loss of region 8 strongly reduced *Sox2-luc* expression relative to the control deletion, whereas reciprocally, ectopic Ars2 activated the control deletion but not the version lacking the Ars2 binding site (Fig. 4c). Therefore, Ars2 activates *Sox2* through promoter region 8. We then incubated NSC nuclear extract with a series of overlapping 90-bp radiolabelled probes covering the ~500 base pairs (bp) of *Sox2* region 8, and observed a specific gel shift of subregion 8-3 (Fig. 4d). This band was completely super-shifted by inclusion of Ars2 antibody, but not Myc antibody (Fig. 4d). We defined the Ars2 binding site more precisely, revealing that Ars2 bound specifically to the central portion of *Sox2* region 8-3 (Fig. 4d). This reflected direct DNA binding activity of Ars2, as *in vitro* translated Ars2 recapitulated specific binding to *Sox2* probe 8-3b (Fig. 4d). This identified a sequence that is highly constrained across mammalian genomes (Fig. 4e and Supplementary Fig. 13).

To determine whether Sox2 mediates Ars2 function *in vivo*, we electroporated *Sox2* expression construct into $Ars2^{\Delta/\Delta}$ postnatal SVZ. Notably, Sox2 rescued the self-renewal and multipotency defects of *Ars2* knockout cells (Fig. 4f–j). By contrast, NSCs derived from $Ars2^{\Delta/\Delta}$ SVZ electroporated with cyclin D1 lacked self-renewal capacity (Fig. 4f) and multipotency (Fig. 4g,k). This confirmed that *Ars2* knockout cells cannot be rescued by driving proliferation. Instead, Ars2 confers NSC identity as a self-renewing cell type by activating *Sox2*.

A central goal of stem-cell biology is to understand the molecular mechanisms that regulate stem-cell self-renewal and multipotency. We show that Ars2 is specifically expressed by NSCs, and not by transit-amplifying progenitors and neuroblasts, and that it maintains the self-renewal and multipotency capacity of postnatal and adult NSCs. In this setting, Ars2 is not required for cell viability, but is instead essential for maintaining core NSC properties. *Ars2* depletion or knockout decreased the NSC pool, decreased neurogenesis and strongly increased non-neurogenic astrocytes. We have assigned a new molecular function for the conserved RNA factor Ars2 as a sequence-specific DNA binding protein, and a critical direct activator of *Sox2* during *in vivo* NSC self-renewal and multipotency. More generally, in light of the interest surrounding the role of Sox2 as a core pluripotency factor in embryonic stem cells and induced pluripotent stem cells, Ars2 may regulate stem-cell self-renewal in these settings as well. This possibility is bolstered by the early embryonic arrest of *Ars2* knockout mice[25], which strongly resembles embryonic arrest in *Sox2* knockout mice[26].

METHODS SUMMARY

All procedures using mice were performed in accordance with the Institutional Animal Care and Use Committee (IACUC). For analysis of adult cells, we injected GFP-expressing Mokola lentivirus (shControl or shArs2) into two different locations of the SVZ using stereotaxic control, and processed brain sections for immunohistochemistry. In addition, we dissected infected SVZs, purified GFP^+ cells and assayed them for self-renewal and multipotency capacity, as described[27]. For conditional knockout analysis, we crossed mice carrying the *Ars2* conditional allele[4] with *hGFAP-Cre* mice. For intraventricular electroporation assays using Split-Cre[11], we used neonatal and P1 $Ars2^{fl/fl}$ pups and killed them 5 days later for self-renewal and multipotency assays. $Dicer1^{\Delta/\Delta}$ and $Drosha^{\Delta/\Delta}$ NSC cultures were generated by transfection with 5 μg of pMSCV-GFP-Cre, and resulting GFP^+ cells were isolated and cultured for 2 weeks before analysis. For chromatin immunoprecipitation, three million NSCs were crosslinked in 1% paraformaldehyde (PFA) and incubated with nuclear lysate and Ars2 antibody. Binding of nuclear extract or in vitro translated Ars2 to radiolabelled Sox2 probes was assayed in 4% tris-borate-EDTA (TBE) gels. All primers used for cloning, ChIP followed by quantitative PCR (ChIP–qPCR) and gel shifts are listed in Supplementary Tables 1–6.

Full Methods and any associated references are available in the online version of the paper at www.nature.com/nature.

Received 2 March; accepted 14 November 2011.
Published online 25 December 2011.

1. Laubinger, S. *et al.* Dual roles of the nuclear cap-binding complex and SERRATE in pre-mRNA splicing and microRNA processing in *Arabidopsis thaliana*. *Proc. Natl Acad. Sci. USA* **105,** 8795–8800 (2008).
2. Lobbes, D., Rallapalli, G., Schmidt, D. D., Martin, C. & Clarke, J. SERRATE: a new player on the plant microRNA scene. *EMBO Rep.* **7,** 1052–1058 (2006).
3. Yang, L., Liu, Z., Lu, F., Dong, A. & Huang, H. SERRATE is a novel nuclear regulator in primary microRNA processing in *Arabidopsis*. *Plant J.* **47,** 841–850 (2006).
4. Gruber, J. J. *et al.* Ars2 links the nuclear cap-binding complex to RNA interference and cell proliferation. *Cell* **138,** 328–339 (2009).
5. Sabin, L. R. *et al.* Ars2 regulates both miRNA- and siRNA-dependent silencing and suppresses RNA virus infection in *Drosophila*. *Cell* **138,** 340–351 (2009).
6. Fuchs, E., Tumbar, T. & Guasch, G. Socializing with the neighbors: stem cells and their niche. *Cell* **116,** 769–778 (2004).
7. Menn, B. *et al.* Origin of oligodendrocytes in the subventricular zone of the adult brain. *J. Neurosci.* **26,** 7907–7918 (2006).
8. Kriegstein, A. & Alvarez-Buylla, A. The glial nature of embryonic and adult neural stem cells. *Annu. Rev. Neurosci.* **32,** 149–184 (2009).
9. Lledo, P. M., Merkle, F. T. & Alvarez-Buylla, A. Origin and function of olfactory bulb interneuron diversity. *Trends Neurosci.* **31,** 392–400 (2008).
10. Shi, Y., Sun, G., Zhao, C. & Stewart, R. Neural stem cell self-renewal. *Crit. Rev. Oncol. Hematol.* **65,** 43–53 (2008).
11. Beckervordersandforth, R. *et al. In vivo* fate mapping and expression analysis reveals molecular hallmarks of prospectively isolated adult neural stem cells. *Cell Stem Cell* **7,** 744–758 (2010).
12. Potten, C. S. Stem cells in gastrointestinal epithelium: numbers, characteristics and death. *Phil. Trans. R. Soc. Lond. B* **353,** 821–830 (1998).
13. Cotsarelis, G., Sun, T. T. & Lavker, R. M. Label-retaining cells reside in the bulge area of pilosebaceous unit: implications for follicular stem cells, hair cycle, and skin carcinogenesis. *Cell* **61,** 1329–1337 (1990).
14. Alonso, M. *et al.* Turning astrocytes from the rostral migratory stream into neurons: a role for the olfactory sensory organ. *J. Neurosci.* **28,** 11089–11102 (2008).
15. Raponi, E. *et al.* S100B expression defines a state in which GFAP-expressing cells lose their neural stem cell potential and acquire a more mature developmental stage. *Glia* **55,** 165–177 (2007).
16. Shi, Y. *et al.* Expression and function of orphan nuclear receptor TLX in adult neural stem cells. *Nature* **427,** 78–83 (2004).
17. Zencak, D. *et al. Bmi1* loss produces an increase in astroglial cells and a decrease in neural stem cell population and proliferation. *J. Neurosci.* **25,** 5774–5783 (2005).
18. Zhuo, L. *et al.* hGFAP-cre transgenic mice for manipulation of glial and neuronal function *in vivo*. *Genesis* **31,** 85–94 (2001).
19. Ohtsuka, T., Sakamoto, M., Guillemot, F. & Kageyama, R. Roles of the basic helix-loop-helix genes *Hes1* and *Hes5* in expansion of neural stem cells of the developing brain. *J. Biol. Chem.* **276,** 30467–30474 (2001).
20. Hitoshi, S. *et al.* Notch pathway molecules are essential for the maintenance, but not the generation, of mammalian neural stem cells. *Genes Dev.* **16,** 846–858 (2002).
21. Ferri, A. L. *et al. Sox2* deficiency causes neurodegeneration and impaired neurogenesis in the adult mouse brain. *Development* **131,** 3805–3819 (2004).
22. Suh, H. *et al.* In vivo fate analysis reveals the multipotent and self-renewal capacities of $Sox2^+$ neural stem cells in the adult hippocampus. *Cell Stem Cell* **1,** 515–528 (2007).
23. Favaro, R. *et al.* Hippocampal development and neural stem cell maintenance require *Sox2*-dependent regulation of *Shh*. *Nature Neurosci.* **12,** 1248–1256 (2009).
24. Ohtsuka, T. *et al.* Visualization of embryonic neural stem cells using Hes promoters in transgenic mice. *Mol. Cell. Neurosci.* **31,** 109–122 (2006).
25. Wilson, M. D. *et al. ARS2* is a conserved eukaryotic gene essential for early mammalian development. *Mol. Cell. Biol.* **28,** 1503–1514 (2008).
26. Avilion, A. A. *et al.* Multipotent cell lineages in early mouse development depend on SOX2 function. *Genes Dev.* **17,** 126–140 (2003).
27. Andreu-Agulló, C., Morante-Redolat, J. M., Delgado, A. C. & Farinas, I. Vascular niche factor PEDF modulates Notch-dependent stemness in the adult subependymal zone. *Nature Neurosci.* **12,** 1514–1523 (2009).

Supplementary Information is linked to the online version of the paper at www.nature.com/nature.

Acknowledgements We thank X. Lu, M. Götz, A. Rizzino, P. M. LLedo, P. Charneau, M. Segura, P. L. Howard and S. Olejniczak for reagents. We are grateful to K. Hadjantonakis, A. Ferrer-Vaquer, J. Zhang and Y. Ganat for assistance. U. Ruthishauser, V. Tabar and the Molecular Cytology Core Facility at the Memorial Sloan-Kettering Cancer Center shared equipment. S. R. Ferron, H. Mira, A. Joyner, H. Duan, Q. Dai, I. Farinas and S. Shi provided critical comments. Work in E.C.L.'s group was supported by the Burroughs Wellcome Fund, the Starr Cancer Consortium (I3-A139) and the NIH (R01-GM083300). C.A.-A. was funded by a EMBO Long-Term Fellowship (ALTF 718-2008) and a NYSTEM Fellowship.

Author Contributions C.A.-A. performed and designed all of the experiments, T.M. performed *in vivo* lentivirus injections and C.B.T. provided reagents. C.A.-A. and E.C.L. conceived the project, interpreted the results and wrote the manuscript.

Author Information Reprints and permissions information is available at www.nature.com/reprints. The authors declare no competing financial interests. Readers are welcome to comment on the online version of this article at www.nature.com/nature. Correspondence and requests for materials should be addressed to C.A.-A. (andreuac@mskcc.org) or E.C.L. (laie@mskcc.org).

METHODS

Mice and genotyping. All mice were housed in the Memorial Sloan-Kettering Cancer Center mouse facility and treated with procedures approved by the Institutional Animal Care and Use Committee (IACUC). For the Ars2 genotyping, the following primers were used: JJG188, 5′-GTTATGCTAGCCCCCAGCCC-3′; JJG189, 5′-GAAGAGAGCAGCGCACCTCC-3′ and JJGdel, 5′-CAGCTTACTA TGGCCCAGCC-3′. JJG188 + JJG189 gives a 300-bp band for the wild-type allele and a 400-bp band for the floxed allele. JJGdel + JJG189 gives a 260-bp band for the deleted allele. Genotyping for *Drosha*[28] and *Dicer1* (ref. 29) was performed as described.

Lentivirus production. We cloned *Ars2* and *Sox2* shRNAs into the third generation lentiviral vector pFUGWH1 (ref. 30). The target sequences used are listed in Supplementary Table 1. The shRNA-expressing lentiviral plasmid was co-transfected with psPAX2 and Mokola G envelope plasmids[31] in 293FT cells. Virus-containing media were collected, filtered and concentrated by ultracentrifugation at 45,000*g* for 2 h, and re-suspended in PBS. Viral titres were measured by serial dilution on NIH3T3 cells followed by flow cytometry analysis after 72 h. The titre of the virus used ranged between 6–9×10^9 plaque forming units per ml.

Lentivirus injection. Mice were anaesthetized with Ketamine (100 mg per kg-, Ketaset) and Xylazine (10 mg per kg, AmTech), and were administered Buprenex (0.05 mg per kg) before being placed on a stereotaxic frame (myNeurolab, Leica). One microlitre of high titre lentiviral vectors (>10^9 plaque forming units per ml) were injected in the subventricular zone (SVZ) of 2- to 4-month-old ICR mice using a microinjector and a 5-µl Hamilton syringe 75RN(32/2"/90 DEG) mounted with a 32 gauge needle. The injection coordinates were optimized according to an injection trial in which mice were injected with a vital dye, the brains were sectioned and the injection site localized. To increase the transduction efficiency of the targeted cell population, we chose to perform two injections at different depths in two different coordinates in the right hemisphere of the brain. The coordinates were (in mm, relative to Bregma and to the surface of the skull, anteroposterior, mediolateral and dorsoventral, respectively) (0.5, 1.1, 2.5–1.7) and (1, 0.9, 3– 2.5). After surgery, mice were given an intraperitoneal injection of saline (1 ml) and were closely monitored until fully ambulatory, and were checked again at 24 h and 48 h after surgery. Experiments were conducted in accordance with NIH and IACUC guidelines and the Research Animal Resources Center approved all of the procedures.

Intraventricular electroporation. Neonatal to postnatal day 1 (P1) *hGFAP-Cre*::*Ars2*$^{fl/fl}$ pups were used to perform intraventricular electroporation, as previously described[32]. For Split-Cre plasmid electroporations[33] a 1/1.5 CCre/NCre vector ratio was used.

Histology. The chlorodeoxyuridine (CldU) administration regime has been described in detail[34]. Mice were anaesthetized with an overdose of Ketamine and Xylazine and transcardially perfused with 4% PFA. Brains were removed and post-fixed in 4% paraformaldehyde (PFA) overnight at 4 °C. A vibratome was used to cut 30-µm coronal sections. The following antibodies were used: rabbit anti-Ars2 (1/25,000; gift of X. Lu), sheep anti-tyrosine hydroxylase (1/1,000; Pel-Freez), rabbit anti-calbindin (1/5,000; Swant), rabbit anti-calretinin (1/1,000; Millipore), mouse anti-β-tubulin (Tuj1) (1/500; Covance), mouse anti-LeX (1/20; BD Pharmigen), rabbit anti-caspase3 (1/100; Cell Signaling Technologies), mouse anti-Mash1 (1/100; BD Pharmigen), goat anti-Sox2 (1/150; R&D Systems), goat anti-Doublecortin (1/500; Santa Cruz), rat anti-CldU (1/600; Accurate), rabbit anti-Ki67 (1/500; Abcam), rat anti-CD133 (Prominin-1) (1/100; eBioscience), mouse anti-nestin (1/200; Millipore), rabbit anti-GFP (1/500; Molecular Probes), mouse anti-GFP (1/500; Molecular Probes) and chicken anti-GFP (1/500; Molecular Probes).

***In vivo* quantification.** A Leica CTR6500 confocal laser-scanning microscope was used for *in vivo* quantification analysis of GFP$^+$ cells. All images were taken using the same pinhole setting (1 µm) and using a ×20 oil objective or a ×40 oil objective. Stacks of optical slices (1 µm thick) were collected through the *z* axis of brain sections of the SVZ and olfactory bulb. For SVZ quantifications, the whole extent of the SVZ (from the rostral tip of the crossing of the corpus callosum and extending caudally to the rostral tip of the crossing of the anterior commissure) was cut in coronal sections (30 µm thick). For double and triple stain analysis, usually a total of 10–15 slices (one every three slices) from each animal were selected. For quantification, the cells situated within 50–60 µm from the lateral wall of the ventricle were counted. For olfactory bulb quantifications, the olfactory bulb (from the rostral tip of the olfactory ventricle to the rostral limit of the accessory olfactory bulb) was sliced in coronal vibratome sections (30 µm thick). Usually 10 slices (one every four slices) from each animal were used. In both cases, co-localization was evaluated in single optical planes taken through the entire *z* axis of each GFP$^+$ cell. Data are expressed as the percentage of double- or triple-labelled GFP$^+$ cells normalized to the total GFP$^+$ cell population. For example, to determine the proliferation rate of GFAP$^+$Sox2$^+$ cells, the number of GFP$^+$GFAP$^+$Sox2$^+$Ki67$^+$ cells was scored and divided by the total number of GFP$^+$ GFAP$^+$Sox2$^+$-expressing cells. See Supplementary Table 2 for details about the number of GFP$^+$ cells that were analysed and the total number of animals that were used in each case.

Plasmid construction. To generate *Sox2-luc*, the 6-kb mouse *Sox2* promoter was PCR amplified from pBSK plasmid (gift of A. Rizzino) using the restriction enzyme-modified PCR primers Sox2_XhoI(F) and Sox2_HindIII(R). To generate Sox2 deletion 5, two fragments were amplified using the following primers: Sox2_XhoI(F), Sox2_del5(R), Sox2_del5(F) and Sox2_HindIII(R). To generate Sox2 deletion 8, two different fragments were PCR amplified from the full-length construct using the following primers: Sox2_XhoI(F) and Sox2_del8(R), Sox2_del8(F), and Sox2_HindIII(R). The fragments were cloned into pGL3-basic vector. Cloning was performed using Cold Fusion Kit (SBI, Systems Biosciences) following the manufacturer's instructions. See Supplementary Table 3 for primer sequences.

Neural stem-cell culture and multipotency assays. ICR mice were purchased from Taconic and neural stem cells (NSCs) were cultured as previously described[7]. Single neurospheres of similar sizes were collected using a pipette and each one was seeded in a single matrigel-coated P-96 well. They were allowed to differentiate for 7 days *in vitro* (2 days in neurosphere medium containing fibroblast growth factor (FGF) and 5 days in 2% fibroblast bovine serum (FBS)). At least 40 clones were analysed per condition. Retrovirus production and *in vitro* infection of NSCs were performed as described[35]. The following antibodies were used: chicken anti-GFAP (1/1,500; Millipore), mouse anti-O4 (1/2; Developmental Studies Hybridoma Bank) and β-III-tubulin (1/300; Covance).

NSC transfection and luciferase assays. NSCs from passages 4 to 8 were grown for 48 h and transfected using Nucleofector (II) (Amaxa Biosystems). A total of 1.5 µg DNA was transfected per well. Fifty nanograms (ng) of a *Renilla* luciferase construct was used as an internal control. Twenty-four to thirty-six hours after electroporation, luciferase activity was measured using Dual-Glo (Promega). For each experiment, each value represents the mean luciferase activity in three different wells and each construct was analysed in three independent experiments. Luciferase activity was normalized to empty vector on the full-length *Sox2-luc*.

Chromatin immunoprecipitation. Cells were crosslinked with 1% formaldehyde at 23 degrees Celsius for 10 min. Glycine was added to a final concentration of 125 mM to stop crosslinking. Cells were rinsed twice with cold PBS and incubated for 10 min at 4 °C in low salt washing buffer (10 mM Tris (pH 8.0), 1 mM EDTA (pH 8.0), 0.5 mM EGTA (pH 8.0), 0.25% Triton X-100, 1 mM PMSF, 1× Complete (Roche)). After centrifugation at 3,500*g*, the pellet was re-suspended in high salt washing buffer (10 mM Tris (pH 8.0), 1 mM EDTA (pH 8.0), 0.5 mM EGTA (pH 8.0), 0.2 M NaCl, 1 mM PMSF, 1× Complete (Roche)) and incubated for 10 min at 4 °C. Nuclei were re-suspended in 1% SDS lysis buffer and chromatin was sonicated to obtain DNA fragments of around 500 bp. One-tenth of total volume was saved for total input DNA control. Lysates were pre-cleared by incubation with 50 µl of Protein A-sepharose (50% slurry pre-blocked with salmon sperm DNA, yeast tRNA and BSA) for 1 h. Immunoprecipitation was performed overnight at 4 °C with 4 µg rabbit anti-Ars2 antibody, 4 µg mouse anti-Ars2 antibody and 4 µg mouse or rabbit IgG. After immunoprecipitation, 60 µl of pre-blocked Protein A-sepharose (50% slurry) was added and the incubation continued for another 4 h. Precipitates were thoroughly washed and extracted twice in 1% SDS and 0.1 M $NaHCO_3$ in TE buffer. Elutes were incubated at 65 °C overnight to reverse crosslinking and then incubated for 1 h at 50 °C with 10 µM EDTA, 40 µM Tris-HCl (pH 6.8) and 20 µg proteinase K (Roche). DNA fragments were recovered by Qiaquick PCR purification kit (Qiagen). Primers that were used are listed in Supplementary Table 4.

Generation of *Dicer1*$^{\Delta/\Delta}$ and *Drosha*$^{\Delta/\Delta}$ NSC cultures. We generated NSC cultures from the SVZ of 2-month-old wild-type, *Dicer1*$^{fl/fl}$ and *Drosha*$^{fl/fl}$ mice. At passage 1, 3 × 10^6 NSCs were transfected with 5 µg of pMSCV-GFP-Cre (Addgene 20781) using Nucleofector (II) (Amaxa Biosystems). Three days later, we isolated GFP$^+$ cells using FACS and cultured NSCs for 2 weeks to allow recombination. After this period the cells were collected for genotyping. Five micrograms of pMSCV-Ars2 or empty pMSCV was transfected to each genotype and after 24 h, cells were plated for a self-renewal assay.

Electrophoretic mobility shift assays. Nuclear extracts were prepared from NSCs as described[36]. For *in vitro* translation, 20 µg of Ars2 cDNA cloned into pcDNA3.1 (gift of P. Howard) or empty vector pcDNA3.1 were subjected to a transcription reaction for 1 h at 32 °C (Pierce) followed by a translation reaction for 90 min at 30 °C using the Human *In vitro* Protein Expression Kit (Pierce), following the manufacturer's instructions. For the binding reaction of the EMSA assays, 8 µg of translated protein was used.

Probes were labelled by incubating 1 µl of forward oligonucleotide (100 ng per µl) with 1 µl of ×10 T4 kinase buffer (New England Biolabs), 1 µl ^{32}P γ-dATP, 1 µl PNK kinase (New England Biolabs) and 6 µl water at 37 °C for 1 h. After adding

90 µl of TE buffer, the forward probe was purified by using Illustra Microspin G-25 columns (GE Healthcare), following the manufacturer's instructions. To anneal oligonucleotides, 5 µl of reverse oligonucleotide (100 ng per µl), 5 µl of 2 M KCl and 90 µl of mQ water were added to the forward labelled probe, and this was boiled for 5 min and cooled down slowly. In each reaction, 1 µl of labelled probe was used. To prepare the unlabelled competitor, 10 µg of forward oligonucleotide and 10 µg of reverse oligonucleotide were incubated with 5 µl of 2 M KCl, and 175 µl of mQ water were added to the forward labelled probe. This was boiled for 5 min and cooled down slowly.

For the binding reaction, 15 µg of nuclear extract, 4 µg of antibody or IgG, 100 ng of labelled probe, 1 µg of poly(dI-dC) and 2 µl of binding buffer (5X) were incubated for 30 min at 23 °C. The binding buffer (5X) contained 375 mM NaCl, 50 mM Tris-HCl pH 7.5, 5 mM EDTA and 30% glycerol. The samples were loaded in a 4% non-denaturing tris-borate-EDTA (TBE) gel that was pre-run for 30 min at 150 V. After 4 h the gel was dried and expose to film using Fujifilm Image Gauge version 4.1. See Supplementary Table 5 for oligonucleotides used in the assay.

RNA isolation and real-time PCR analysis. Total RNA was isolated using Trizol (Invitrogen) and 1 µg of total RNA was used to synthesize complementary DNA using random primers and reverse transcriptase (SuperScript II RT; Invitrogen). For quantitative PCR, SYBR PCR Master Mix (Applied Biosystems) was used in a CFX96 Real-Time System thermocycler (Biorad). Primers that were used are listed on Supplementary Table 6.

Statistical analysis. Data are always shown as mean values ± s.e.m. Analyses of significant differences between means were performed using two-tailed Student's *t*-tests. The arcsen transformation for normalization was applied to relative values (fold-change and percentage). *n*, number of independent cultures or animals used. In all cases $*P < 0.05$; $**P < 0.01$; $***P < 0.005$.

28. Chong, M. M., Rasmussen, J. P., Rudensky, A. Y. & Littman, D. R. The RNAseIII enzyme Drosha is critical in T cells for preventing lethal inflammatory disease. *J. Exp. Med.* **205,** 2005–2017 (2008).
29. Harfe, B. D., McManus, M. T., Mansfield, J. H., Hornstein, E. & Tabin, C. J. The RNaseIII enzyme *Dicer* is required for morphogenesis but not patterning of the vertebrate limb. *Proc. Natl Acad. Sci. USA* **102,** 10898–10903 (2005).
30. Ivanova, N. *et al.* Dissecting self-renewal in stem cells with RNA interference. *Nature* **442,** 533–538 (2006).
31. Alonso, M. *et al.* Turning astrocytes from the rostral migratory stream into neurons: a role for the olfactory sensory organ. *J. Neurosci.* **28,** 11089–11102 (2008).
32. Boutin, C., Diestel, S., Desoeuvre, A., Tiveron, M. C. & Cremer, H. Efficient in vivo electroporation of the postnatal rodent forebrain. *PLoS ONE* **3,** e1883 (2008).
33. Beckervordersandforth, R. *et al.* In vivo fate mapping and expression analysis reveals molecular hallmarks of prospectively isolated adult neural stem cells. *Cell Stem Cell* **7,** 744–758 (2010).
34. Ferrón, S. R. *et al.* A combined *ex/in vivo* assay to detect effects of exogenously added factors in neural stem cells. *Nature Protocols* **2,** 849–859 (2007).
35. Andreu-Agulló, C., Morante-Redolat, J. M., Delgado, A. C. & Farinas, I. Vascular niche factor PEDF modulates Notch-dependent stemness in the adult subependymal zone. *Nature Neurosci.* **12,** 1514–1523 (2009).
36. Whitman, M. C. & Greer, C. A. Synaptic integration of adult-generated olfactory bulb granule cells: basal axodendritic centrifugal input precedes apical dendrodendritic local circuits. *J. Neurosci.* **27,** 9951–9961 (2007).